

Geophysical Research Letters*



RESEARCH LETTER

10.1029/2024GL108761

Key Points:

- New numerical models with convergent velocity boundary condition for deciphering subduction polarity during arc-continent collisions
- Thrust faults, metamorphic rocks, magmatism, topography and Moho morphology can be used as indicators to diagnose subduction polarity
- The evolution of subduction polarity reversal well explains the tectonic activities of the Kamchatka and Banda Arc in the Cenozoic

Supporting Information:

Supporting Information may be found in the online version of this article.

Correspondence to:

Z. Yan, yanzyphd@mail.iggcas.ac.cn

Citation

Yan, Z., Chen, L., Zuza, A. V., Xiang, X., Xie, R., & Ai, S. (2024). Deciphering subduction polarity during ancient arc-continent collisions. *Geophysical Research Letters*, *51*, e2024GL108761. https://doi.org/10.1029/2024GL108761

Received 8 FEB 2024 Accepted 29 JUL 2024

Author Contributions:

Conceptualization: Lin Chen Investigation: Zhiyong Yan Methodology: Zhiyong Yan, Lin Chen Supervision: Lin Chen Visualization: Zhiyong Yan, Xiao Xiang

Writing – original draft: Zhiyong Yan Writing – review & editing: Zhiyong Yan, Lin Chen, Andrew V. Zuza, Xiao Xiang, Renxian Xie, Sanxi Ai

© 2024. The Author(s).

This is an open access article under the terms of the Creative Commons

Attribution-NonCommercial-NoDerivs

License, which permits use and distribution in any medium, provided the original work is properly cited, the use is non-commercial and no modifications or adaptations are made.

Deciphering Subduction Polarity During Ancient Arc- Continent Collisions

Zhiyong Yan¹, Lin Chen¹, Andrew V. Zuza², Xiao Xiang^{1,3}, Renxian Xie⁴, and Sanxi Ai⁵

¹State Key Laboratory of Lithospheric and Environmental Coevolution, Institute of Geology and Geophysics, Chinese Academy of Sciences, Beijing, China, ²Nevada Bureau of Mines and Geology, Nevada Geosciences, University of Nevada, Reno, NV, USA, ³College of Earth and Planetary Sciences, University of Chinese Academy of Sciences, Beijing, China, ⁴School of Transportation Engineering, East China Jiaotong University, Nanchang, China, ⁵Hubei Subsurface Multi-Scale Imaging Key Laboratory, School of Geophysics and Geomatics, China University of Geosciences, Wuhan, China

Abstract The closure of an ancient ocean basin via oceanic arc-continent collision has two subduction styles with opposite polarities, which may proceed via subduction polarity reversal (SPR) or a subduction zone jump (SZJ). Interpreting the geometry or kinematic evolution of ancient collisional zones, especially the original subduction polarity, can be challenging. Here we used 2D thermo-mechanical modeling to investigate the dynamic evolution process of SPR versus SZJ. Our modeling predicts different structural, topographic, magmatic, and basin histories for SPR and SZJ, which can be compared against, and help interpret, the geologic record past sites of oceanic closure during collisional orogens. Our results match geologic observations of past collisions in Kamchatka, eastern Russia, and the Banda Arc, eastern Indonesia, and thus our results can help effectively decode the evolutionary history of past arc-continent collisions.

Plain Language Summary Determining the geometry and kinematic evolution of ancient subduction zones that experienced collision with an oceanic island arc can be challenging based on the surface geology along. Such collisions usually result in different dynamical evolution processes, namely subduction polarity reversal (SPR) or a subduction zone jump (SZJ). Here we conducted numerical modeling of oceanic island arcs that collide with a continental margin to explore the dynamic evolution process of different subduction styles. Our results reveal geologic indicators to decipher SPR versus SZJ in natural oceanic arccontinent collisions, such as the distribution of thrust faults, metamorphic rocks, magmatism, crustal thickness, and topography. The numerical simulations help explain the geologic history of Kamchatka in eastern Russia and Banda Arc in eastern Indonesia. This study provides provide new insights and implications diagnosing the polarity of vanished subduction in arc-continental systems.

1. Introduction

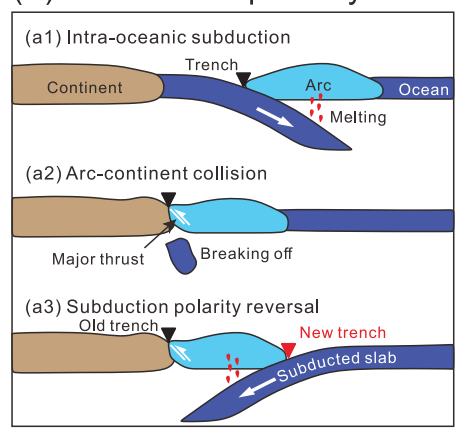
Intra-oceanic island arcs are widely distributed across the oceans, with along-strike lengths of 100–1000s km and across-strike widths of up to 100s km (Stern, 2010; Tetreault & Buiter, 2014). Their typical crustal thickness and density—20–35 km and 2,790 kg/m³ respectively—are much thicker and less dense than the surrounding oceanic crust, which results in their resistance to subduction and accretion onto continental margins during ocean-closure events that generates ophiolite belts at the collisional zone (e.g., Stern, 2010; Tetreault & Buiter, 2014; and references therein). Arc-continent collisions have been well documented in accretional orogens such as those in the SW Pacific or the Caribbean (e.g., Brown et al., 2011; Cloos, 1993; Stern, 2010; Tetreault & Buiter, 2014). The arc-continental collisional process may induce subduction initiation (SI) such as inferred for Kamchatka in eastern Russia (e.g., Clift et al., 2003; Draut & Clift, 2013; Plunder et al., 2020; Stern, 2004, 2010; Yang, 2022). There are two distinct SI mechanisms that can occur, depending on the subduction polarity before arc-continent collision: subduction polarity reversal (SPR) or a subduction zone jump (SZJ) (Figure 1).

It can be challenging to properly interpret the subduction polarity before arc-continent collision through examination of exposed ophiolitic rocks, as both SPR and SZJ can lead to the consumption and disappearance of the oceanic crust between the arc and continent and the final emplacement of ophiolites at the surface. Furthermore, in the ancient geologic record, the polarity of the initial subduction zone cannot be directly observed, and thus it must be inferred from geological, geochemical, or geophysical observations. Diagnosing the polarity of extinct subduction can help to understand the role of plate driving forces and the dynamic mechanisms of SI, especially

YAN ET AL. 1 of 10

19448007, 2024, 15, Downloaded from https://agupubs.onlinelibrary.wiley.com/doi/10.1029/2024GL108761 by University Of Nevada Reno, Wiley Online Library on [14/03/2025]. See the Terms

conditions) on Wiley Online Library for rules of use; OA articles are governed by the



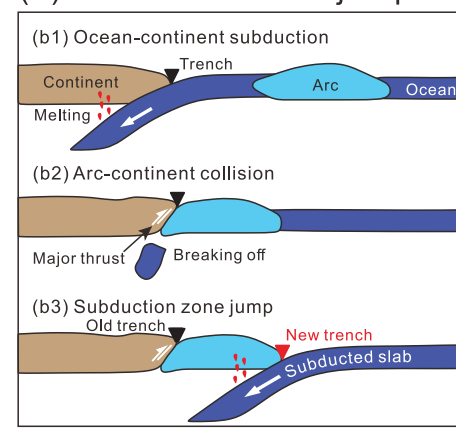


Figure 1. Two distinct types of subduction initiation induced by arc-continent collision. (a) Subduction polarity reversal, and (b) subduction zone jump.

the origin of intra-oceanic SI, which is of great significance to understanding plate tectonic activities. However, the identification of the polarity of an ancient subduction zone can be complex (e.g., Plunder et al., 2020; Yang, 2022). This leads to an important question of how to diagnose subduction polarity during ancient arccontinent collision, which can be investigated by assessing the dynamic process of arc-continent collision using numerical simulations.

Past studies this topic have mainly focused on the accretion of island arcs and the growth process of continents (e.g., Brown et al., 2006, 2011; Cloos, 1993; Stern, 2010; Tetreault & Buiter, 2012, 2014), the dynamics of collision-induced SI along buoyant blocks (i.e., island arcs or oceanic plateaus) (e.g., Almeida et al., 2022; Dong et al., 2022; Stern & Gerya, 2018; Sun et al., 2021; Wang et al., 2022; Yan et al., 2021), or the dynamic mechanism of SPR induced by intra-oceanic arc (e.g., Zhang & Leng, 2021). To our knowledge, of the past research on intra-oceanic arcs, none have yet considered the dynamic processes that lead to accretion via different subduction polarities (Figure 1), such as subduction within the ocean (Figure 1a1) or at the continental margin (Figure 1b1). Furthermore, such numerical simulations can help us better understand diagnostic characteristics to better interpret SPR or SZJ in the geologic observations.

To address these issues, here we designed two-dimensional models to explore the dynamic arc-continent collision process. First, we recovered the dynamic evolution of two different subduction polarities (SPR vs. SZJ) during arc-continent collision by systematically testing the width and thickness of the arcs, their surrounding sediments, and plate convergence rates. We then examined patterns of deformation, modeled pressure-temperature (P-T) paths, magmatism, and topography from the different models to determine which indicators are key identifiers for diagnosing subduction polarity. Finally, we diagnose geological examples using the indicators predicted by our models, providing new insights into decoding ancient extinct subduction zones.

2. Numerical Methods

Our numerical simulations are based on the 2D geodynamical code I2VIS (Gerya & Yuen, 2003), which uses staggered grid finite difference method and maker-in-cell technique to solve the mass, momentum, and energy conservation equations. The full details of the method can be found in Gerya (2010).

2.1. Numerical Geometry

The model is 4,000 km wide and 1,000 km deep (Figure 2). The right side of the model is the continental plate, and the left side is the oceanic plate, where an island arc with thickened crust and variable width is embedded. Island arcs are typically located ~120 km inboard from the trench (Tetreault & Buiter, 2014). The term island arc here refers to either the relic of intra-oceanic subduction with arc magmatism or an oceanic plateau with similar properties to the island arc, both of which were originally located far away from the continental margin (e.g., Dong et al., 2022; Tetreault & Buiter, 2012). To capture the intra-oceanic subduction process prior to arc-

YAN ET AL. 2 of 10

19448007, 2024, 15, Downloaded from https://agupubs.onlinelibrary.wiley.com/doi/10.1029/2024GL108761 by University Of Nevada Reno, Wiley Online Library on [14/03/2025]. See the Terms and Conditions (https://onlinelibrar

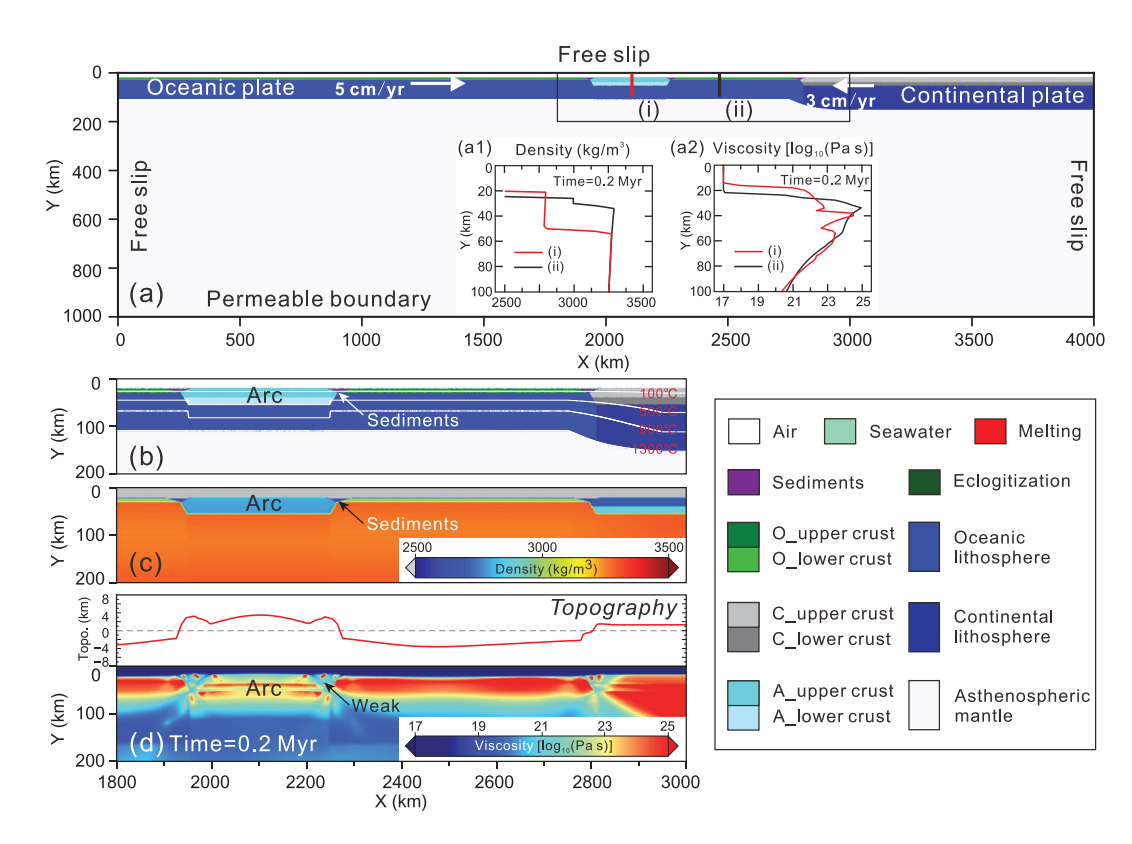


Figure 2. Model setup. (a) The composition field of reference model setup (a1, a2) Density and viscosity profiles beneath the arc (i) and oceanic lithosphere (ii) at 0.2 Myr (b)–(d) Zoomed area of interest showing the detailed structure of composition, density, topography and viscosity, respectively. The white solid lines denote isotherms.

continent collision, we set the arc 650 km away from the continental margin in our model. The thickness of sediment in the transition zone between ocean and continent is up to 10 km, and the thickness and viscosity of sediments around the island arc vary. The density of the arc is 2,800 kg/m³ (Tetreault & Buiter, 2014), which is lighter than the oceanic crust. The oceanic crust is 8 km thick, including 3 km thick of upper crust and 5 km thick of lower crust, and the lithospheric thickness is defined by oceanic age. The continental lithosphere is 140 km thick, including a 20 km thick of upper crust, a 15 km thick of lower crust, and a 105 km thick of lithospheric mantle.

2.2. Initial Boundary Conditions

The temperatures at the upper and lower model boundaries are set to 0 and 1,790°C, respectively. The oceanic lithosphere temperature is described by the half-space cooling model (Turcotte & Schubert, 2002). Our model defines the oceanic plate as a laterally homogeneous plate with an age of 40 Ma, except for the island arc, which has a linear temperature profile. A "sticky air" layer is placed on top of the model to simulate the evolution of surface elevation (Schmeling et al., 2008), which is 20 km thick above the continental plate and arc and 22 km thick above the oceanic plate. Viscous flow laws are derived from Ranalli (1995) and are shown in Table S1 in Supporting Information S1. The upper, left, and right boundaries have free-slip boundary conditions, whereas the lower boundary is permeable (Burg & Gerya, 2005). The bottom interface of the lithosphere is 1,300°C. The initial velocities at oceanic (X = 1,200 km) and continental (X = 3,200 km) plates are set at 5 cm/yr and 3 cm/yr, respectively, except for models specifically stating velocity tests. The detailed material properties used in the study are presented in Table S2 in Supporting Information S1.

3. Model Results and Discussions

We conducted a total of 59 numerical experiments (Table S3 in Supporting Information S1), and obtained subduction scenarios located around island arc and at the ocean-continent transition zone (Figure S1; see Text S1

YAN ET AL. 3 of 10

in Supporting Information S1 for details). Here we focus on the dynamic process of SPR and SZJ during the arccontinent collision.

Herein we define the onset of subduction as when the frontmost edge of the subducting plate is beneath the overriding plate. Therefore, the duration of SPR starts from the arc-continent collision to the new SI. We define the pro-side of the island arc as the side closest to the continental margin and the retro-side is farther from the continental margin.

3.1. Reference Models for SPR and SZJ

Figure 3 shows two subduction processes of different polarities, SPR and SZJ. In the SPR model (Model 1 in Table S3 in Supporting Information S1), the arc has a crustal thickness of 35 km and a width of 300 km. In this case, subduction first starts at the pro-side of the intra-oceanic arc, forming partial melting of oceanic crust (Figure 3a1). As the trench continues to retreat, magmatism migrates to the continental margin, until the ocean between the arc and continent is completely closed, and the arc finally collides with the continent at ~8.0 Myr (Figure S2a in Supporting Information S1; Movie S1). It is accompanied by the migration of high topography caused by the compressed arc (Figure 3a1) toward the continental margin (Figure 3a4). As the arc was accreted and thrust onto the continental margin, a new subduction zone of opposite polarity formed on the retro-side of the arc with continued convergence at 11.5 Myr (i.e., SPR), and the subduction-related magmatism jumped to the side away from the continental margin (Figure 3a2). The duration of the SPR is ~3.5 Myr (Figure S2a in Supporting Information S1). The retro-arc subduction and shallow underthrusting of the continental plate formed a bivergent wedge structure and an intracontinental basin behind the continental margin (Figure 3a2, 3a4).

In contrast, the SI in the SZJ mode (Model 16 with the arc of 30-km-thick and 400-km-wide in Table S3; Figure S2b in Supporting Information S1) first starts at the continental margin, where the trench remains, and subduction-related magmatism acts on the overriding continent (Figure 3b1; Movie S2). Then the proto-oceanic arc is almost entirely accreted onto the continental margin, and subduction-related magmatism jumps with SZJ to the retro-side of the arc (Figure 3b2). The accreted arc and subducting oceanic slab have the same tendency toward the Moho (Figure 3b2). The overriding continent is thrust on the arc, resulting in wholescale uplifted topography across the collisional zone with no inland sedimentary basin (Figure 3b4).

We selected four markers in Model 1 to track the P-T paths of upper and lower crust of the continental margin and the arc close to the continental margin, as shown in Figure 3a3. The upper (black point) and lower (red point) crustal markers of the arc experienced similar trajectories. Although the early evolution was complicated, their temperature and pressure dropped from the beginning to the last moment, corresponding to the thrust process. Conversely, the markers of the overriding continental upper (purple point) and lower (green point) crust experienced a rapid pressure increase in the early stage and nearly isobaric heating in the later stage, corresponding to the early subduction and later stagnation process of the continental margin. High-pressure metamorphism occurred in the upper and lower crust of the continent. Similarly, we tracked P-T paths of four markers in Model 16 (Figure 3b3). The markers in the arc upper (black point) and lower (red point) crust first experienced a process of increasing pressure and temperature, and then a process of decreasing pressure, corresponding to the subduction and exhumation processes of the frontal arc materials, respectively. The pressure of the markers of the overriding continental upper (purple point) and lower (green point) crust does not change much. The source area of ultrahigh-pressure metamorphic rock is intra-oceanic arc material.

3.2. Results for Other Models

Several models have static subduction zones with no arc-continent collision and no induced SI (Figure S1 in Supporting Information S1). For example, Model 17 (Figure S3 in Supporting Information S1) involves subduction starting on the retro-side of the island arc and Model 5 (Figure S4 in Supporting Information S1) has subduction remaining constant along the continental margin. In either case, there is no discernible migration of magmatism and topography at the continental margin only experiences a small uplift (Figures S3, S4 in Supporting Information S1). In most ocean-continent subduction models (style B in Figure S1 in Supporting Information S1), the arcs are subducted into the asthenosphere along with oceanic slab, and only a small part of the crust is scraped and accreted on the continental margins, as shown in Model 5 (Figure S4 in Supporting Information S1). This type of model subduction-related magmatism occurs only at trenches along continental margin.

YAN ET AL. 4 of 10

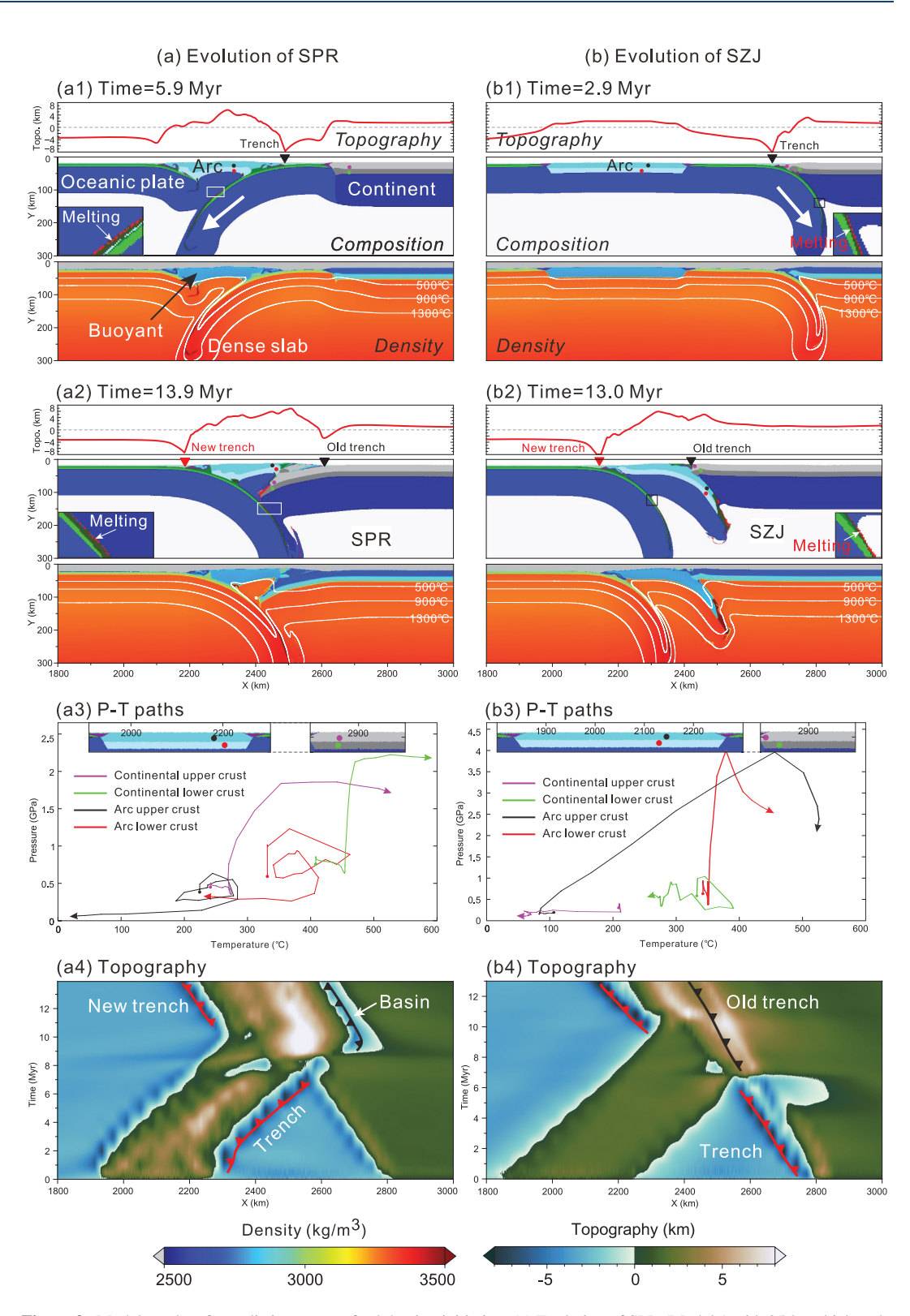


Figure 3. Model results of two distinct types of subduction initiation. (a) Evolution of SPR (Model 1 with 35-km-thick and 300-km-wide). (b) Evolution of SZJ (Model 16 with 30-km-thick and 400-km-wide) (1, 2) Evolutionary slices of topography, composition and density, respectively. The white solid lines in figures denote isotherms. (3) The P-T paths show the evolution of arc and continental upper and lower crustal rocks. Location of trackers shown in the composition field. (4) Topographical evolution. SPR, subduction polarity reversal. SZJ, subduction zone jump.

YAN ET AL. 5 of 10

3.3. Indicators for Diagnosing Subduction Polarity

Here, based on our model results, we demonstrate how the subduction polarity can be identified based on indicators such as thrust faults, metamorphic rocks, topography, Moho geometry, and subduction-related magmatism.

In the model of SPR (e.g., Model 1; Figure 3a), the arc collided with the continental margin and was thrust onto the continent, forming an accretionary complex containing oceanic crust, sediments, and arc crust at the continental margin. High-pressure metamorphism occurred within the continental crust, and a sedimentary basin was formed behind the continental margin due to the downward thrusting of the continental crust. A bivergent wedge structure including the Moho formed in the collision zone due to the retro-arc subduction and downward thrusting of the continental plate. Subduction-related magmatism first impacted the intra-oceanic arc, and migrated to the continental margin as the trench retreated, then jumped away from the margin as the retro-arc subduction started.

In the model of SZJ (e.g., Model 16; Figure 3b), the ultrahigh-pressure metamorphic rocks were derived from intra-oceanic arc materials because the continental plate was thrust over the island arc and the island arc had a downward subducting tendency. As a result, the Moho interface of the island arc and the retro-arc subducting oceanic slab have the same dip toward the continental margin. An inland basin was not formed. Unlike the SPR model, subduction-related magmatism in the SZJ model occurred along the continental margin before arccontinent collision and then migrated onto the oceanic arc.

3.4. Implications for Diagnosing Geological Events

The SPR or SZJ processes are inferred in many geologic settings (e.g., Advokaat et al., 2018; Harris, 2011; Konstantinovskaia, 2001; Suppe, 1984; Wan et al., 2019; Yang, 2022). Here, we discuss how the Banda Arc in eastern Indonesia and Kamchatka in eastern Russia are two areas (Figure 4a) where SPR is likely to occur after arc-continent collision based on the indicators of our model. Thrust faults recorded in the Timor Trough provide evidence that the Banda Arc may be undergoing SPR (Figure 4b). The collision between the Banda Arc and the Australian Plate occurred ca. 8–10 Ma (Keep & Haig, 2010; Tate et al., 2014, 2015). Thrusting initiated in the Timor orogen at ca. 4.5 Ma (Tate et al., 2014, 2015) as evidenced by Wetar Thrust activity (Harris, 2011). It takes about 5 Myr for the Banda arc to develop SPR after the collision with the Australian plate. To the west of Timor Trough, the Indian Ocean lithosphere is subducting northward under the Sunda Arc, and the SPR is also reversed on the north side of the Sunda Arc, which was recorded by Flores Thrust (Silver et al., 1983).

The Kamchatka orogenic belt is located at the junction of the Pacific Plate, North American Plate, and Eurasian Plate (Figure 4a). It is composed of multiple units, including the Kamchatka terrane and Sredinny accretionary complex in the west, the Olyutorsky intra-oceanic arc thrust on the Kamchatka terrane in the middle, and the Vetlovsky accretionary wedge and Kronotsky arc in the east (Figure 4c; Konstantinovskaia, 2001; Hourigan et al., 2009; Konstantinovskaya, 2011; Vaes et al., 2019). Based on metamorphic rock and zircon ages, the collision time between the Olyutorsky arc and southern Kamchatka is constrained to 55-52 Ma (Bindeman et al., 2002; Hourigan et al., 2009; Kirmasov et al., 2004; Luchitskaya et al., 2008; Luchitskaya & Soloviev, 2012; Shapiro et al., 2008). Furthermore, the age of the sedimentary layers below the suture and the age of the undeformed overlapping sequence and the age of the granodiorite suture zone constrain the collision time of the Olyutorsky arc with northern Kamchatka to be ca. 45 Ma (Garver et al., 2000; Solov'ev et al., 2002, 2011). This indicates that there was an ancient eastward subduction and that the collision of the Kamchatka and Olyutorsky Arc was completed ca. 45 Ma. The eastern Vetlovsky accretionary prism lies beneath the Olyutorsky arc and is separated by a northwest-dipping thrust fault. Combined with the fact that this thrust fault is unconformably covered by middle Eocene mudstones and sandstones and the timing of the emplacement of the Kronotsky arc, the onset of westward subduction can be constrained to the late Early Eocene (Solov'ev et al., 2004; Hourigan et al., 2009; Konstantinovskaya, 2011; Domeier et al., 2017). The SPR of the Kamchatka orogen occurred about 10 Ma after the collision of the Olyutorsky arc and Kamchatka.

Although the results of our two-dimensional model cannot reflect the spatiotemporal sequence of the north-south tectonic evolution of the Kamchatka orogenic belt, our model reproduces the dynamics process of the east-west SPR induced by the collision of Olyutorsky arc and Kamchatka (Figure 4d). Our model shows that the oceanic slab initially subducted toward the intra-oceanic arc, the ocean closed and then the arc collided with the continental margin (Figure S2a in Supporting Information S1). This process corresponds to the eastward oceanic

YAN ET AL. 6 of 10

19448007, 2024, 15, Downloaded from https://agupubs.onlinelibrary.wiley.com/doi/10.1029/2024GL108761 by University Of Nevada Reno, Wiley Online Library on [14/03/2025]. See the Terms and Conditions (https://onlinelibrary.wiley.com/term

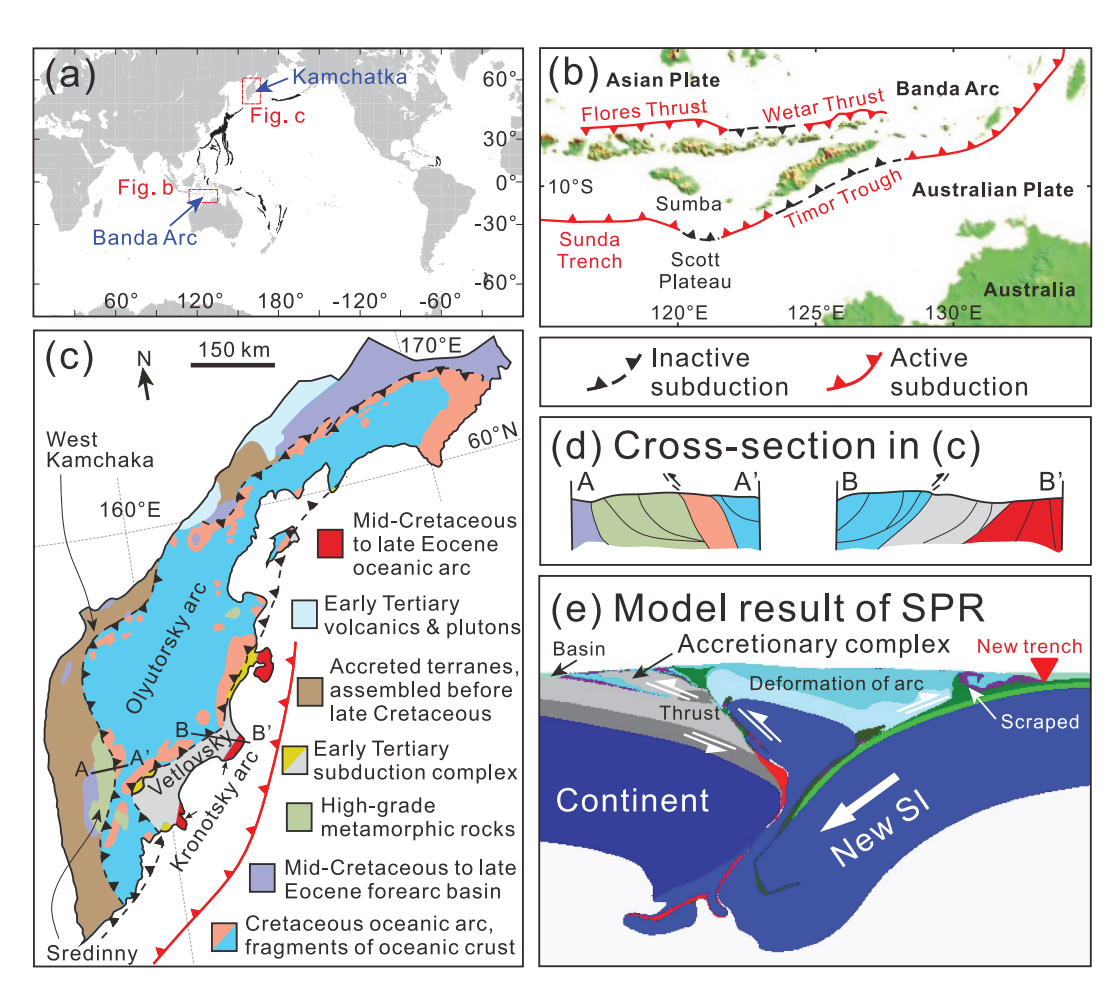


Figure 4. Comparison of model results of SPR with geological examples. (a) Global location map of intra-oceanic arc systems shown in black (modified after Tetreault & Buiter, 2014), and two possible regions of SPR. (b) Tectonic map showing the major tectonic units around the Sunda-Banda Arc. (c) Generalized tectonic map of the Kamchatka Peninsula. The position of (b) and (c) are shown in the red dotted box in Fig. a (modified after Yang, 2022). (d) Cross-sections of Kamchatka in Fig. c refer to Brown et al. (2011). (e) Model result of SPR (Model 1) at 12.0 Myr. SPR, subduction polarity reversal.

subduction, and the subsequent collision of the Olyutorsky arc with the Kamchatka terrane (e.g., section AA' in Figure 4d). With continuous convergence, the intra-oceanic arc thrust over the continent, forming complex accretionary prisms comprised of sediments and oceanic crust accreted from the subducted oceanic plate, and island arc materials (Figures 3a and 4e), which is well reflected in the Sredinny complex in the Kamchatka, including granulite, amphibolite, migmatite and granite (Figure 4c; Konstantinovskaia, 2001). In addition, our model also reproduces the evolution of intracontinental basins in this region well (Figures 4c–4e). Finally, the SPR occurred on the other side of the arc, accompanied by subduction-related magmatism, a process corresponding to westward subduction in the late Early Eocene, emplacement of the Vetlovsky accretionary prism and the Kronotsky arc process (e.g., section BB' in Figure 4d). In addition, the duration of SPR predicted by our results is 2–12 Myr (Figure S5 in Supporting Information S1), which also matches the observed geologic timescale of SPR in the Kamchatka orogenic belt (ca. 10 Myr).

4. Model Limitations

Numerical simulation is an effective tool for simulating dynamic processes, especially for recovering the evolution of ancient subduction zones, which helps us infer past dynamic processes based on existing surface response observations. Here, to understand how different subduction polarities (SPR vs. SZJ) affect the observable geological record of collision, we simplified the model design and imposed a continuous convergence-

YAN ET AL. 7 of 10

onditions) on Wiley Online Library for rules of use; OA articles are governed by the applicable Creativ

Acknowledgments

We thank Taras Gerya for providing the

I2VIS code. We would like to thank the

comments and suggestions, which greatly

improved the presentation of the paper. We

also thank Editor Christian Huber and

editorial work. ZY wishes to thank Shi

discussion in the 345 office. This study

was supported by the NSFC (42204099)

and the U.S. National Science Foundation

(EAR 2210074). All the models were run

on the Beijing Super Cloud Computing Center and on the Supercomputing

Laboratory, IGGCAS in Beijing.

Yao, Tongtong Xie and Lixue Ma for the

Associate Editor for their excellent

two reviewers for their constructive

induced subduction. However, recent studies have highlighted the large differences in behavior between incipient and steady-state subduction (e.g., Chen et al., 2015), and the slab bending radius and hinge dissipation factors have different effects on the overriding plate at different subduction stages (Irvine & Schellart, 2012). In addition, recent 3D numerical models of buoyancy-driven subduction emphasized that the size and timing of the subduction zone affect the deformation of the overriding plate (Schellart, 2024). Therefore, in the future, it may be necessary to more systematically study the dynamic behavior of arc-continent collisions under different scenarios such as free subduction boundary conditions, incipient and steady-state subduction, and use 3D simulations to fully understand the typical characteristics of different ancient subduction polarities.

5. Conclusions

We systematically explored the dynamic process during arc-continent collisions through numerical simulations, providing a reference of diagnostic indicators for deciphering the subduction polarity of ancient subduction systems. Subduction polarity can be identified based on indicators such as thrust faults, metamorphic rocks, subduction-related magmatism, topography, and Moho geometry. Our SPR model results well explain the Cenozoic SPR tectonic event in the Kamchatka orogenic belt from west to east and the tectonic evolution process of the Banda Arc in eastern Indonesia. Our numerical model provides new insights and implications for deciphering ancient subduction polarity.

Conflict of Interest

The authors declare no conflicts of interest relevant to this study.

Data Availability Statement

All the figures were generated with Generic Mapping Tools https://www.generic-mapping-tools.org/ (Wessel et al., 2019). All related data of numerical models are available in an online data repository, https://doi.org/10.5281/zenodo.10605350 (Yan, Chen, Zuza, et al., 2024) or can be requested by contacting the authors.

References

- Advokaat, E. L., Bongers, M. L. M., Rudyawan, A., BouDagher-Fadel, M. K., Lan-gereis, C. G., & van Hinsbergen, D. J. J. (2018). Early cretaceous origin of the Woyla Arc (Sumatra, Indonesia) on the Australian plate. Earth and Planetary Science Letters, 498, 348–361. https://doi.org/10.1016/j.epsl.2018.07.001
- Almeida, J., Riel, N., Rosas, F. M., Duarte, J. C., & Schellart, W. P. (2022). Polarity-reversal subduction zone initiation triggered by buoyant plateau obstruction. *Earth and Planetary Science Letters*, 577, 117195. https://doi.org/10.1016/j.epsl.2021.117195
- Bindeman, I. N., Vinogradov, V. I., Valley, J. W., Wooden, J. L., & Natal'in, B. A. (2002). Archean protolith and accretion of crust in Kamchatka: SHRIMP dating of zircons from Sredinny and Ganal Massifs. *The Journal of Geology*, 110(3), 271–289. https://doi.org/10.1086/339532
- Brown, D., Ryan, P. D., Afonso, J. C., Boutelier, D., Burg, J. P., Byrne, T., et al. (2011). Arc-continent collision: The making of an orogen. Frontiers of Earth Science, 4, 477–493.
- Brown, D., Spadea, P., Puchkov, V., Alvarez-Marron, J., Herrington, R., Willner, A. P., et al. (2006). Arc-Continent collision in the southern Urals. Earth-Science Reviews, 79(3–4), 261–287. https://doi.org/10.1016/j.earscirev.2006.08.003
- Burg, J., & Gerya, T. (2005). The role of viscous heating in Barrovian metamorphism of collisional orogens: Thermomechanical models and application to the Lepontine Dome in the central alps. *Journal of Metamorphic Geology*, 23(2), 75–95. https://doi.org/10.1111/j.1525-1314. 2005.00563.x
- Chen, Z., Schellart, W., & Duarte, J. (2015). Overriding plate deformation and variability of fore-arc deformation during subduction: Insight from geodynamic models and application to the Calabria subduction zone. *Geochemistry, Geophysics, Geosystems*, 16(10), 3697–3715. https://doi.org/10.1002/2015gc005958
- Clift, P. D., Schouten, H., & Draut, A. E. (2003). A general model of arc-continent collision and subduction polarity reversal from Taiwan and the Irish Caledonides. Geological Society, London, Special Publications, 219(1), 81–98. https://doi.org/10.1144/gsl.sp.2003.219.01.04
- Cloos, M. (1993). Lithospheric buoyancy and collisional orogenesis: Subduction of oceanic plateaus, continental margins, island arcs, spreading ridges, and seamounts. *The Geological Society of America Bulletin*, 105(6), 715–737. https://doi.org/10.1130/0016-7606(1993)105<0715: lbacos>2.3.co;2
- Domeier, M., Shephard, G. E., Jakob, J., Gaina, C., Doubrovine, P. V., & Torsvik, T. H. (2017). Intraoceanic subduction spanned the Pacific in the late cretaceous-Paleocene. *Science Advances*, 3(11), eaao2303. https://doi.org/10.1126/sciadv.aao2303
- Dong, H., Dai, L., Liu, L., Jiang, X., Li, S., Gong, W., et al. (2022). Joint geodynamic-geophysical inversion suggests passive subduction and accretion of the Ontong Java plateau. *Geophysical Research Letters*, 49(23), e2022GL100744. https://doi.org/10.1029/2022gl100744
- Draut, A. E., & Clift, P. D. (2013). Differential preservation in the geologic record of intraoceanic arc sedimentary and tectonic processes. *Earth-Science Reviews*, 116, 57–84. https://doi.org/10.1016/j.earscirev.2012.11.003
- Garver, J. I., Soloviev, A. V., Bullen, M. E., & Brandon, M. T. (2000). Towards a more complete record of magmatism and exhumation in continental arcs, using detrital fission-track thermochrometry. *Physics and Chemistry of the Earth*, 25(6–7), 565–570. https://doi.org/10.1016/ s1464-1895(00)00086-7
- Gerya, T. V. (2010). Introduction to numerical geodynamic modelling. Cambridge University Press.

YAN ET AL. 8 of 10



Geophysical Research Letters

- 10.1029/2024GL108761
- Gerya, T. V., & Yuen, D. A. (2003). Characteristics-based marker-in-cell method with conservative finite-differences schemes for modeling geological flows with strongly variable transport properties. *Physics of the Earth and Planetary Interiors*, 140(4), 293–318. https://doi.org/10.1016/j.pepi.2003.09.006
- Harris, R. (2011). The nature of the Banda arc-continental collion in the Timor region. In D. Brown & P. D. Ryan (Eds.), *Arc-continent collision.* Frontiers in Earth sciences (pp. 163–211). Springer-Verlag.
- Hourigan, J. K., Brandon, M. T., Soloviev, A. V., Kirmasov, A. B., Garver, J. I., Stevenson, J., & Reiners, P. W. (2009). Eocene arc-continent collision and crustal consolidation in Kamchatka, Russian Far East. American Journal of Science, 309(5), 333–396. https://doi.org/10.2475/05.2009.01
- Irvine, D. N., & Schellart, W. P. (2012). Effect of plate thickness on bending radius and energy dissipation at the subduction zone hinge. *Journal of Geophysical Research*, 117(6), 1. https://doi.org/10.1029/2011jb009113
- Keep, M., & Haig, D. W. (2010). Deformation and exhumation in Timor: Distinct stages of a young orogeny. *Tectonophysics*, 483(1–2), 93–111. https://doi.org/10.1016/j.tecto.2009.11.018
- Kirmasov, A., Solov'ev, A., & Hourigan, J. (2004). Collision and postcollision structural evolution of the Andrianovka suture, Sredinny Range, Kamchatka. *Geotectonics*, 38, 294–316.
- Konstantinovskaia, E. A. (2001). Arc-continent collision and subduction reversal in the Cenozoic evolution of the Northwest Pacific: An example from Kamchatka (NE Russia). *Tectonophysics*, 333(1–2), 75–94. https://doi.org/10.1016/s0040-1951(00)00268-7
- Konstantinovskaya, E. (2011). Early eocene arc–continent collision in Kamchatka, Russia: Structural evolution and geodynamic model. Frontiers in Earth Science, 4, 247–277. Springer Berlin Heidelberg. https://doi.org/10.1007/978-3-540-88558-0_9
- Luchitskaya, M. V., Solov'ev, A. V., & Hourigan, J. K. (2008). Two stages of granite formation in the Sredinny Range, Kamchatka: Tectonic and geodynamic setting of granitic rocks. *Geotectonics*, 42(4), 286–304. https://doi.org/10.1134/s0016852108040031
- Luchitskaya, M. V., & Soloviev, A. V. (2012). Early eocene magmatism in the Sredinnyi Range, Kamchatka: Composition and geodynamic aspects. *Petrology*, 20(2), 147–187. https://doi.org/10.1134/s0869591112020038
- Plunder, A., Bandyopadhyay, D., Ganerød, M., Advokaat, E. L., Ghosh, B., Bandopadhyay, P., & van Hinsbergen, D. J. J. (2020). History of subduction polarity reversal during arc-continent collision: Constraints from the Andaman ophiolite and its metamorphic sole. *Tectonics*, 39(6), e2019TC005762. https://doi.org/10.1029/2019tc005762
- Ranalli, G. (1995). Rheology of the earth. Chapman and Hall.
- Schellart, W. P. (2024). Subduction dynamics and overriding plate deformation. Earth-Science Reviews, 253, 104755. https://doi.org/10.1016/j.earscirev.2024.104755
- Schmeling, H., Babeyko, A. Y., Enns, A., Faccenna, C., Funiciello, F., Gerya, T. V., et al. (2008). A benchmark comparison of spontaneous subduction models-towards a free surface. *Physics of the Earth and Planetary Interiors*, 171(1–4), 198–223. https://doi.org/10.1016/j.pepi. 2008.06.028
- Shapiro, M. N., Solov'ev, A. V., & Hourigan, J. K. (2008). Lateral structural variability in zone of eocene island-arc-continent collision, Kamchatka. Geotectonics, 42(6), 469–487. https://doi.org/10.1134/s0016852108060046
- Silver, E. A., Reed, D., McCaffrey, R., & Joyodiwiryo, Y. (1983). Back arc thrusting in the eastern Sunda Arc, Indonesia: A consequence of arccontinent collision. *Journal of Geophysical Research*, 88(B9), 7429–7448. https://doi.org/10.1029/jb088ib09p07429
- Solov'ev, A., Garver, J. I., Shapiro, M. N., Brandon, M. T., & Hourigan, J. K. (2011). Eocene arc-Continent collision in northern Kamchatka, Russian far east. Russ. *Journal of Earth Sciences*, 12, 1–13.
- Solov'ev, A., Shapiro, M., & Garver, J. (2002). Lesnaya nappe, northern Kamchatka. Geotectonics, 36, 469-482.
- Solov'ev, A., Shapiro, M., Garver, J., & Lander, A. (2004). Formation of the east Kamchatkan accretionary prism based on fission-track dating of detrital zircons from terrigene rocks. Russian Geology and Geophysics, 45, 1237–1247.
- Stern, R. J. (2004). Subduction initiation: Spontaneous and induced. Earth and Planetary Science Letters, 226(3–4), 275–292. https://doi.org/10.1016/j.epsl.2004.08.007
- Stern, R. J. (2010). The anatomy and ontogeny of modern intra-oceanic arc systems. *Geological Society*, 338(1), 7–34. https://doi.org/10.1144/sp338.2
- Stern, R. J., & Gerya, T. (2018). Subduction initiation in nature and models: A review. *Tectonophysics*, 746, 173–198. https://doi.org/10.1016/j.
- Sun, B., Kaus, B. J., Yang, J., Lu, G., Wang, X., Wang, K., & Zhao, L. (2021). Subduction polarity reversal triggered by oceanic plateau accretion: Implications for induced subduction initiation. Geophysical Research Letters, 48(24), e2021GL095299. https://doi.org/10.1029/2021gl095299
- Suppe, J. (1984). Kinematics of arc-continent collision flipping of subduction, and back-arc spreading near Taiwan. *Memoir of the Geological Society of China*, 6(21), V33.
- Tate, G. W., McQuarrie, N., van Hinsbergen, D. J. J., Bakker, R. R., Harris, R., & Jiang, H. (2015). Australia going down under: Quantifying continental subduction during arc-continent accretion in Timor-Leste. *Geosphere*, 11(6), 1860–1883. https://doi.org/10.1130/ges01144.1
- Tate, G. W., McQuarrie, N., van Hinsbergen, D. J. J., Bakker, R. R., Harris, R., Willett, S., et al. (2014). Resolving spatial heterogeneities in exhumation and surface uplift in Timor-Leste: Constraints on deformation processes in young orogens. *Tectonics*, 33(6), 1089–1112. https://doi.org/10.1002/2013tc003436
- Tetreault, J. L., & Buiter, S. J. H. (2012). Geodynamic models of terrane accretion: Testing the fate of island arcs, oceanic plateaus, and continental fragments in subduction zones. *Journal of Geophysical Research*, 117(B8). https://doi.org/10.1029/2012jb009316
- Tetreault, J. L., & Buiter, S. J. H. (2014). Future accreted terranes: A compilation of island arcs, oceanic plateaus, submarine ridges, seamounts, and continental fragments. Solid Earth, 5(2), 1243–1275. https://doi.org/10.5194/se-5-1243-2014
- Turcotte, D. L., & Schubert, G. (2002). Geodynamics (Vol. 484). Cambridge University Press.
- Vaes, B., van Hinsbergen, D. J. J., & Boschman, L. M. (2019). Reconstruction of subduction and back-arc spreading in the NW Pacific and Aleutian basin: Clues to causes of cretaceous and eocene plate reorganizations. *Tectonics*, 38(4), 1367–1413. https://doi.org/10.1029/ 2018tc005164
- Wan, B., Wu, F. Y., Chen, L., Zhao, L., Liang, X. F., Xiao, W. J., & Zhu, R. (2019). Cyclical one-way continental rupture-drift in the Tethyan evolution: Subduction-driven plate tectonics. Science China Earth Sciences, 62(12), 2005–2016. https://doi.org/10.1007/s11430-019-9393-4
- Wang, L., Dai, L., Gong, W., Li, S., Jiang, X., Foulger, G., et al. (2022). Subduction initiation at the Solomon back-arc basin: Contributions from both island arc rheological strength and oceanic plateau collision. *Geophysical Research Letters*, 49(3), e2021GL093369. https://doi.org/10.1029/2021gl097666
- Wessel, P., Luis, J. F., Uieda, L., Scharroo, R., Wobbe, F., Smith, W. H. F., & Tian, D. (2019). The generic mapping Tools version 6. Geochemistry, Geophysics, Geosystems, 20(11), 5556–5564. https://doi.org/10.1029/2019gc008515
- Yan, Z., Chen, L., Xiong, X., Wan, B., & Xu, H. (2021). Oceanic plateau and subduction zone jump: Two-Dimensional thermomechanical modeling. *Journal of Geophysical Research: Solid Earth*, 126(7), e2021JB021855. https://doi.org/10.1029/2021jb021855

YAN ET AL. 9 of 10



Geophysical Research Letters

10.1029/2024GL108761

- Yan, Z., Chen, L., Zuza, A., Xiang, X., Xie, R., & Ai, S. (2024). Deciphering subduction polarity during Ancient Arc-Continent collisions. [Dataset]. Zenodo. https://doi.org/10.5281/zenodo.10605350
- Yang, G. (2022). Subduction initiation triggered by collision: A review based on examples and models. Earth-Science Reviews, 232, 104129. https://doi.org/10.1016/j.earscirev.2022.104129
- Zhang, S., & Leng, W. (2021). Subduction polarity reversal: Induced or spontaneous? Geophysical Research Letters, 48(11), e2021GL093201. https://doi.org/10.1029/2021g1093201

References From the Supporting Information

- Behr, W. M., & Becker, T. W. (2018). Sediment control on subduction plate speeds. Earth and Planetary Science Letters, 502, 166–173. https://doi.org/10.1016/j.epsl.2018.08.057
- Bittner, D., & Schmeling, H. (1995). Numerical modeling of melting processes and induced diapirism in the lower crust. *Geophysical Journal International*, 123(1), 59–70. https://doi.org/10.1111/j.1365-246x.1995.tb06661.x
- Clauser, C., & Huenges, E. (1995). Thermal conductivity of rocks and minerals. In T. J. Ahrens (Ed.), Rock physics and phase relations (Vol. 3, pp. 105–126). American Geophysical Union, Reference Shelf. https://doi.org/10.1029/rf003p0105
- Cloetingh, S., Wortel, R., & Vlaar, N. J. (1982). Evolution of passive continental margins and initiation of subduction zones. *Nature*, 297(5862), 139–142. https://doi.org/10.1038/297139a0
- Erickson, S. G. (1993). Sedimentary loading, lithospheric flexure, and subduction initiation at passive margins. *Geology*, 21(2), 125–128. https://doi.org/10.1130/0091-7613(1993)021<0125:sllfas>2.3.co;2
- Fyfe, W. S., & Leonardos, Jr., O. H. (1977). Speculations on the causes of crustal rifting and subduction, with applications to the Atlantic margin of Brazil. *Tectonophysics*, 42(1), 29–36. https://doi.org/10.1016/0040-1951(77)90015-4
- Lallemand, S., Heuret, A., & Boutelier, D. (2005). On the relationships between slab dip, back-arc stress, upper plate absolute motion, and crustal nature in subduction zones. *Geochemistry, Geophysics, Geosystems*, 6(9), Q09006. https://doi.org/10.1029/2005gc000917
- Schmidt, M. W., & Poli, S. (1998). Experimentally based water budgets for dehydrating slabs and consequences for arc magma generation. *Earth and Planetary Science Letters*, 163(1–4), 361–379. https://doi.org/10.1016/s0012-821x(98)00142-3
- Yan, Z., Chen, L., Zuza, A., & Meng, Q. (2024). Successive accretions of future allochthonous terranes and multiple subduction zone jumps: Implications for Tethyan evolution. *The Geological Society of America Bulletin*, 136(7–8), 3230–3242. https://doi.org/10.1130/B37263.1
- Yan, Z., Chen, L., Zuza, A., Tang, J., Wan, B., & Meng, Q. (2022). The fate of oceanic plateaus: Subduction versus accretion. *Geophysical Journal International*, 231(2), 1349–1362. https://doi.org/10.1093/gjji/ggac266

YAN ET AL. 10 of 10